

Membrane-Based Sensing Approaches

Julia Braunagel,^A Ann Junghans,^A and Ingo Köper^{A,B,C}

^AMax Planck Institute for Polymer Research, 55128 Mainz, Germany.

^BSchool of Chemical and Physical Sciences, Flinders University, Adelaide, SA 5001, Australia.

^CCorresponding author. Email: ingo.koeper@flinders.edu.au

Tethered bilayer lipid membranes can be used as model platforms to host membrane proteins or membrane-active peptides, which can act as transducers in sensing applications. Here we present the synthesis and characterization of a valinomycin derivative, a depsipeptide that has been functionalized to serve as a redox probe in a lipid bilayer. In addition, we discuss the influence of the molecular structure of the lipid bilayer on its ability to host proteins. By using electrical impedance techniques as well as neutron scattering experiments, a clear correlation between the packing density of the lipids forming the membrane and its ability to host membrane proteins could be shown.

Manuscript received: 20 September 2010.

Manuscript accepted: 19 October 2010.

Introduction

Applications in pharmacy, environmental control, or security require more and more sensitive detection methods to probe minute amounts of analyte. Therefore, a wide range of different sensing approaches has been developed. One possibility is to mimic concepts developed in nature. Bilayer membrane-based sensing approaches have the advantage of ideally providing a highly sensitive detection system.^[1–4] In such a system, a membrane protein is embedded in a lipid bilayer and serves as the actual sensing unit. The fragile nature of a membrane protein, however, requires a sophisticated architecture to ensure its proper function. Typically, transmembrane proteins are embedded in a lipid bilayer, often composed of a variety of different lipids. Such lipid mixtures are generally too complex to be used in practical applications. Therefore, several biomimetic model systems have been developed, including vesicular systems, lipid monolayers at the air–water interface, or other model membrane systems. Among these, solid supported membranes and in particular tethered bilayer lipid membranes (tBLM) have been established as useful architectures.^[5–8] They provide a stable and robust sensing platform, where membrane proteins can be incorporated. The general concept of a solid supported membrane consists of a lipid bilayer that is linked to a solid support.^[9] This linkage can be either physical, for example, through electrostatic interactions, or chemical through covalent bonds. Interactions between the lipid bilayer and the solid support can disturb the natural behaviour of the lipid layer, for example, hinder diffusion of lipids and embedded proteins or even lead to denaturation of such proteins. In order to minimize these interactions, various models have been proposed to lift the bilayer off the substrate. One possibility is to insert a polymer cushion between the inner leaflet of the membrane and the solid support.^[10,11] Such systems have been shown to provide excellent membrane fluidity and allow for the functional incorporation of membrane proteins. The disadvantages of a

thick polymer layer, however, are often decreased electrical properties of the bilayer, when compared with natural membranes. Yet, a high resistance of the membrane itself and a low capacitance are essential when the membrane is to be used to host ion channel proteins and to allow for the recording of transport processes through those proteins. Typical ion channel recordings can be made by either using patch clamp systems on whole cells or by using planar bilayer lipid membrane (BLM) systems.^[12] These approaches have been significantly improved in the past years in order to enhance the stability of the fragile bilayer membrane, for example, by the construction of automated patch clamp systems,^[13] or by embedding planar BLM in supporting hydrogels.^[14] Yet, tBLM have been shown to provide the most stable architectures.^[15] A tBLM consists in principle of a lipid bilayer (Fig. 1). The inner leaflet is covalently grafted to a solid support through a spacer moiety.^[16] These anchor lipids thus consist of three parts, a lipid group, a spacer unit, and an anchor group, to allow for the assembly on a solid substrate. Typically, short oligomeric poly(ethylene glycol) units have been used. This spacer part separates the bilayer from the substrate and provides a reservoir underneath the membrane, where electrolytes can diffuse in. Several systems have been proposed, with branched hydrocarbon chains in the lipid part; typical lipids have branched hydrocarbon units, which are in a fluid phase at ambient conditions.^[1,17,18] The anchor unit provides a covalent linkage of the membrane to the substrate. A gold surface is commonly used as substrate, allowing for electrical and optical characterization of the system.^[19–21] For such surfaces, thiol moieties are ideal binding groups. In addition, silanes have been employed to anchor membranes to oxide surfaces, or phosphonate groups for alumina substrates.^[22] The membrane architecture has been studied in detail using various surface analytical techniques, including surface plasmon resonance (SPR) spectroscopy,^[23] electrochemical impedance spectroscopy (EIS),^[24] quartz crystal microbalance, atomic

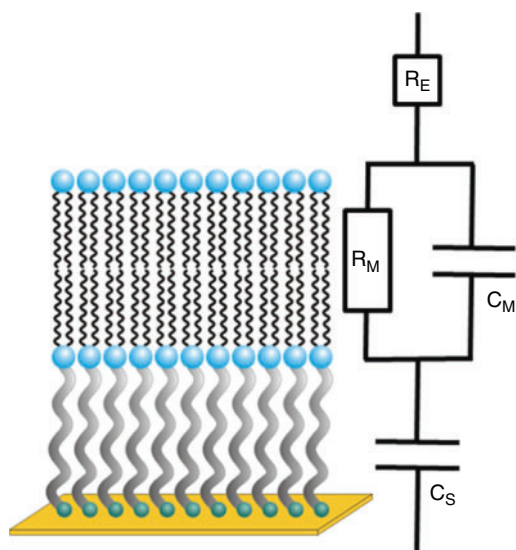


Fig. 1. Schematic depiction of the tethered membrane architecture. The inner leaflet is covalently bound to a substrate by a spacer unit; the distal layer is typically formed by vesicle fusion.^[25] The electrical properties of the membrane can be modelled by a simple equivalent circuit.

force microscopy (AFM),^[25] infrared spectroscopy,^[26] and neutron reflectivity (NR).^[27]

The membrane architecture has been shown to be stable over extended periods of time up to several months.^[28] At the same time, the system provides a biomimetic layer with a high electrical resistance, close to values of the natural analogue.^[23] Various peptides and proteins, especially ion channels, have already been successfully incorporated in a tBLM platform.^[1,5,29]

Here, we will concentrate on two different aspects of the membrane. First, the synthesis of a novel ionophore, which, embedded in a tBLM, can be used as a redox sensor, will be discussed. In the second part, we will discuss the influence of the membrane structure on its ability to host membrane proteins.

Ferrocene–Valinomycin as a Redox Sensor

Valinomycin is an ion carrier that has been widely studied in model membrane systems,^[30–32] however, it has not been used for explicit sensing purposes. The cyclic depsipeptide transports potassium ions highly selectively across a membrane by complexation with its six ester carbonyl groups. The cation is buried inside the cavity of the ionophore, which can diffuse through lipid membranes by exposing multiple hydrophobic side-chains and release the ion at the other side. Natural valinomycin consists of two amino acids (L- and D-valine) and two α -hydroxy acids (L-lactic acid and D-hydroxyisovaleric acid). It has a cyclic structure (c(L-Val-D-Hyiv-D-Val-L-Lac)₃) and is usually isolated from *Streptomyces fulvissimus*.^[33]

The first synthesis of valinomycin was described by Shemyakin et al.^[34] Furthermore, the exchange of one or two amino or hydroxy acids did not significantly alter the transport properties of the molecule.^[35–37] By exchange of one L-valine by an L-lysine a free amino group can be introduced to which different ligands can be coupled through a peptide bond. Through this ligand, an additional functionality can be incorporated into the molecule, for example, a control over the membrane permeability.

Here, ferrocene has been coupled to valinomycin and the modified ion carrier has been investigated in a tBLM architecture. The ferrocene/ferrocinium system is a highly reversible one electron redox pair that creates a positive charge by oxidation, even beyond a water–oil interface.^[38] The thus created positive charge, which is exposed to the solvent, hinders the membrane permeation of the ferrocene–valinomycin. This process is reversible when a reducing agent is added. The system might be used as membrane-based redox sensor.

Experimental

Synthesis of Ferrocene–Valinomycin

The synthesis of the ferrocene–valinomycin (Fig. 2) required various reactions, which will be described in terms of standard operation procedures (SOP). If not stated otherwise, the reaction progress was followed by TLC, and column chromatography was performed after each step. The purity of the products was verified by TLC, HPLC, and NMR spectroscopy.

SOP 1: Didepsides were obtained by reaction of a Boc-protected amino acid (1 equiv.) and a benzyl- or allyl-protected hydroxy acid (1 equiv.) with 4-dimethylaminopyridine (DMAP, 0.1 equiv.) and *N,N'*-dicyclohexylcarbodiimide (DCC, 1.1 equiv.) in dichloromethane (DCM) at -40°C for 12 h.^[39]

SOP 2: Depsipeptides were obtained by reaction of a fragment with a free carboxylic acid (1 equiv.) and a fragment with the free amino acid (1 equiv.) with DMAP (0.1 equiv.) and DCC (1.1 equiv.) in DCM at room temperature (RT) for 12 h.

SOP 3 (Boc-deprotection): The Boc-protected amino fragment was stirred for 2 h in DCM/trifluoroacetic acid (TFA) (4/1) and washed with NaHCO_3 solution. Solvents were removed under vacuum and the crude product was used in the next step without further purification.

SOP 4 (benzyl-deprotection): The benzyl-protected carbonic acid fragment was stirred for 3 h in methanol with Pd/C and hydrogen at RT. The catalyst was removed by filtration, solvents were removed under vacuum, and the crude product was used in the next step without further purification.

Compounds **2** and **6** were obtained with yields of 85% and 67% by reaction of hydroxyisovaleric acid (**1**) with benzyl and allyl bromide (1.1 equiv.), respectively, potassium carbonate (1 equiv.) and potassium iodide (0.1 equiv.) in *N,N*-dimethylformamide (DMF) at RT for 24 h. The didepsides **4**, **5**, and **15** were prepared following SOP 1 with high yields (91–97%). The following deprotection steps were carried out quantitatively according to SOP 3 and 4. The tetradepsipeptide **9** was synthesized according to SOP 2 with a yield of 70%. Fifty percent of the product was benzyl-deprotected (**10**, SOP 4) and the other half was Boc-deprotected (**11**, SOP 3). Both products were coupled with a 76% yield to the octadepsipeptide **12**. Compound **12** was Boc-deprotected and bound to benzyl-deprotected **4** according to SOP 2. The yield for the decadepsipeptide **13** was 60%.

Ferrocene carbonic acid (**16**, 1 equiv.) was activated with oxalyl chloride (2.5 equiv.) in tetrachloromethane at RT for 2 h to give ferrocene acid chloride (**17**). Compound **17** was directly added to a cooled solution of **18** (1 equiv.) in DCM with *N,N*-diisopropylethylamine (DIPEA, 2.5 equiv.) and DMAP (0.1 equiv.) and stirred for 2 h at RT. The yield for **19** was 16%. Compound **19** was stirred in 20% piperidine (DMF) for 2 h, the Fmoc-deprotected didepside **20** was then coupled to the benzyl-deprotected **14** (27% yield). The linear dodecadepsipeptide **21** was allyl-deprotected with $\text{Pd}(\text{PPh}_3)_4$ (0.1 equiv.) and phenyl silane (2 equiv.) in dry DCM under argon for 2 h at RT.

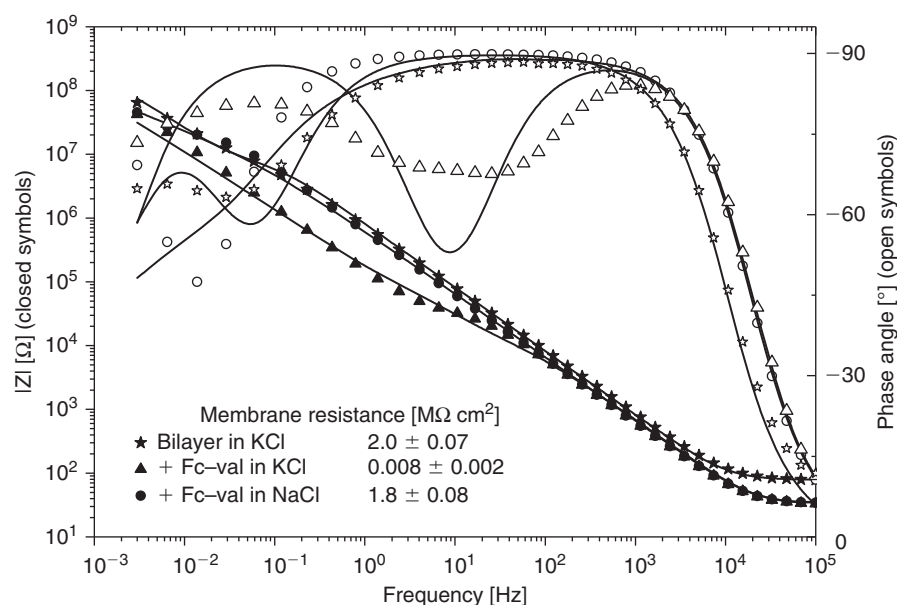


Fig. 3. Bode plot showing a bilayer with incorporated ferrocene–valinomycin. Solid symbols show the impedance data (left axis) and open symbols the phase angle (right axis). Solid lines represent fits of the experimental data using an R(RC)(RC) equivalent circuit, the obtained fitting parameters including fitting errors are listed. After incorporation of valinomycin, a decrease in resistance because of K^+ transport was observed. Transport could be suppressed by rinsing with NaCl, and recovery of the original resistance was measured.

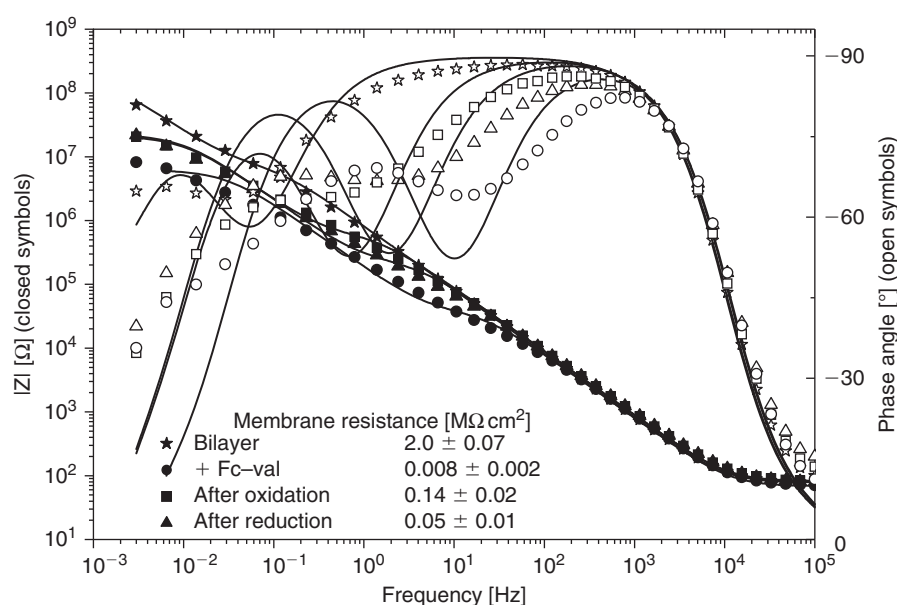


Fig. 4. Bode plot showing a bilayer with incorporated ferrocene–valinomycin. After incorporation of valinomycin a decrease in resistance attributable to K^+ transport was observed. Transport could be hindered by oxidation of the ferrocene ligand with 0.1 M $FeCl_3$. A reduction of the ferrocenium ion was also possible and led to a higher ion transport again.

In order to stop the ion transport through a peptide-functionalized membrane, the ferrocene was oxidized with 0.1 M $FeCl_3$ for 24 h, resulting in an increase in resistance to $0.14 M\Omega cm^2$ (Fig. 4). The positive charge on the ion carrier seemed to hinder the transmembrane movement. There might be the possibility that the charged depsipeptide could leave the bilayer, which would also lead to the observed changes in electrical properties. However, in that case we would expect a more pronounced effect. Furthermore, the process could be

reversed by the addition of 0.1 M hydroquinone (+0.1 M KCl) for 24 h to the system. The resistance then again decreased to $0.05 M\Omega cm^2$.

The novel compound might be used in a redox sensor concept, where the ferrocene unit is used as a switch that allows or permits ion transport. The system would thus be a logic gate (AND operation) with the redox status of ferrocene and the presence of potassium ions as input channels, while the output would be the ion flow. Yet, a reaction time of 24 h is definitely

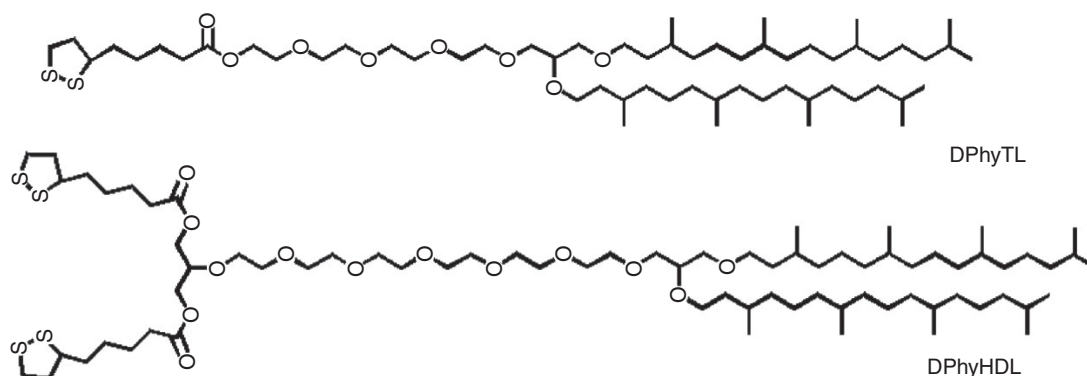


Fig. 5. Structures of the anchor lipids DPhyTL and DPhyHDL.

not suitable for a viable sensor. This time span is attributable to the fact that the molecules have to cross a water–membrane barrier. However, the aim of this research was to show a proof of concept for the system. Further optimization and modification would be needed to enhance the reaction time of the molecules.

Structure–Function Relationship of tBLM

The structure of a tBLM is composed of three distinct parts, the hydrophobic lipid layer, the spacer part, and the anchor moiety. All parts have a certain influence on the final structure and properties of the bilayer architecture.

The assembly of a tBLM is typically a two-step process. First, the anchor lipids bind to a suitable substrate and form a monolayer. For gold substrates, this is typically a self-assembly process, which can be easily followed by various surface analytical tools. Alternatively, and especially for oxidic substrates using silane anchors, the transfer of a lipid film which has been pre-arranged at the air–water interface can be a suitable deposition method.^[42,43]

For the self-assembly processes, different timescales have been observed, depending on the technique utilized. For example, the formation of the monolayer takes about 3 h, when monitored optically using SPR. When studied in more detail using EIS or AFM, it has been shown that it takes up to 24 h until the monolayer is completely formed and any defects are filled.^[25] Similarly, the completion of the monolayer to a full membrane in the second step, which is typically done by fusion with small unilamellar vesicles, is finished optically much faster than electrically. This is probably a result of rearrangements happening within the membrane, even after the fusion of the vesicles.

In particular, the structure of the anchor lipid itself also has a significant influence on the properties of the formed tBLM. In most cases, phytanoyl moieties have been used. These archae-analogue lipid structures have low transition temperatures, providing fluid membrane architectures at ambient conditions. Furthermore, the branched chains lead to a strong interaction between the hydrophobic chains, resulting in a relatively dense packing.^[42] The spacer group is supposed to lift off the bilayer from the substrate and to provide an electrolyte reservoir underneath the membrane. The lateral structure of the membrane, i.e., the molecular details of the lipid assembly, will have a significant influence on the properties of the bilayer itself.

tBLM have been used to incorporate ion channel proteins and study their function. Therefore, the lipid bilayer should have a high electrical resistance, to ensure that observed transport processes are only attributable to protein function and not to

defects in the membrane. These electrical properties can be easily analyzed using EIS. By comparing different molecular structures of the anchor lipid their influence on the membrane properties can be probed.

We have studied the molecular structure and the resulting membrane properties of two distinctive anchor lipids (Fig. 5).^[44] Both DPhyTL and DPhyHDL consist of two phytanoyl chains as the hydrophobic part. The spacer part consists of a tetra- or hexa-ethylene glycol unit, respectively. While DPhyTL is anchored to the substrate by a single lipoic acid group, two units are used for DPhyHDL. The rationale for the structures is that DPhyTL has been shown to form very densely packed layers,^[23] which might obstruct the incorporation of large membrane proteins. The two anchor groups in DPhyHDL should lead to a more diluted packing in the inner leaflet of the bilayer and underneath the membrane, thus generating more space for proteins to integrate and function. This strategy is an alternative to the use of small molecules as diluting units in the lipid monolayer.^[45,46]

The more branched structure of DPhyHDL should lead to a looser packing of the lipid monolayer. This should have a significant effect on the structural properties and on the ability to host membrane proteins.^[47,48] This hypothesis has been addressed using EIS and NR studies.^[27,44]

NR is an ideal tool to study soft interfaces such as the tBLM architectures. The technique offers the unique opportunity to analyze individually the structures of the different layers of a tBLM system, i.e., the spacer region and the lipid layer. The properties of the spacer part are of special interest. This part should not only lift off the lipid bilayer from the underlying substrate, but also provide an ion reservoir to enable the function of membrane proteins and also accommodate extra-membrane parts of the proteins. Thus it is interesting to analyze how thick the ethylene glycol part of the layer effectively is and how much water can be incorporated. Furthermore, NR allows differences in the tBLM structures to be probed, when the molecular structure of the anchor lipids is modified.

NR experiments have been performed using DPhyTL and DPhyHDL-based membranes (Fig. 6).^[15,27] In order to create a signal with a sufficient intensity, membranes had to be prepared on 3 inch (7.62 cm) silicon wafers as substrates, which have been coated with a thin gold film.

The obtained experimental data could be analyzed in terms of a layer model, with distinctive differences in the scattering length density for the spacer part, and the inner and the outer bilayer leaflet. The results of NR scattering experiments are often presented as scattering length density (SLD) profiles, where the SLD corresponds to the isotopic composition at a certain distance from the substrate surface. In the present case,

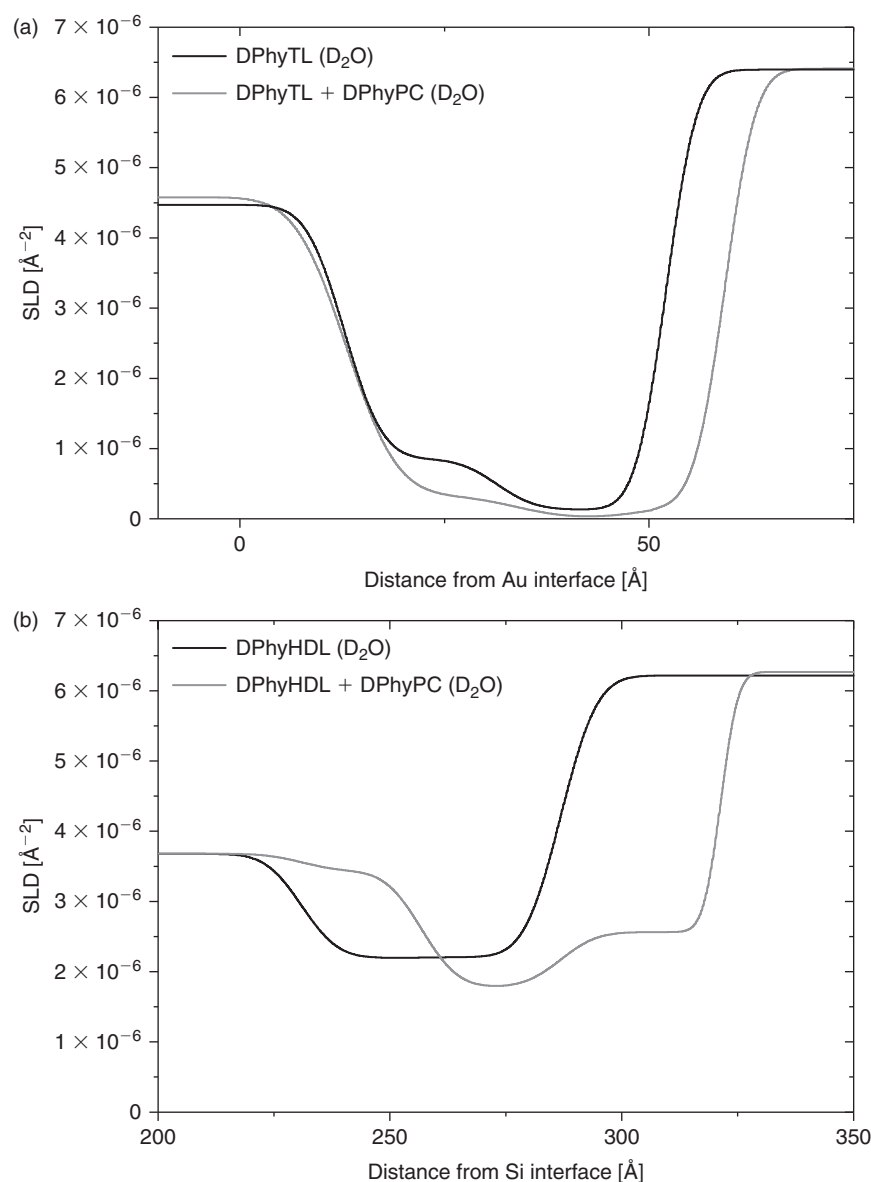


Fig. 6. Neutron reflectivity profiles for (a) DPhyTL and (b) DPhyHDL based membranes. Measurements have been conducted in heavy water for mono- and bilayer assemblies. SLD, scattering length density.

the substrate was a gold film sputtered onto a silicon wafer. Thus the profile plots the composition of the membrane perpendicular to the gold interface (Fig. 6). By using the difference in the SLD of protons and deuterons, different contrasts can be created and specific parts of the molecular architecture analyzed. For example, it was interesting to evaluate the amount of water incorporated into the spacer part of the anchor lipids. Furthermore, the packing density of the lipids was of interest, since these parameters should have a direct influence on the ability of the created tBLM to host membrane proteins. Here, the profiles for DPhyTL show a very high packing density in the lipid region, both for the anchor lipids as well as for the lipids completing the bilayer structure. Similarly, the SLD of the spacer region is relatively high for a polymer layer and the difference in SLD for measurements in D_2O and a mixture of D_2O and H_2O showed that the spacer part contained only $\sim 5\%$ water. In contrast to these values, the DPhyHDL membrane showed a much looser structure. The lipid density was increased, which indicated a more diluted packing of the lipid chains. In

addition, a relatively high amount of water was incorporated in the spacer region ($\sim 65\%$) and even in the alkyl part of the membrane. The anchor lipid containing the two lipoic acid groups as anchor moieties thus led to a more diluted membrane structure. This had a significant influence on the electrical properties of the membranes as well as on the ability to host membrane proteins, here the ion channel α -hemolysin.

The electrical properties of a DPhyHDL-based membrane showed significantly different values from those obtained for a DPhyTL-based bilayer (Fig. 7). While resistance values up to $20\text{ M}\Omega\text{ cm}^2$ have been reported for DPhyTL, the anchor lipid with the larger anchor group led to maximum values of $\sim 1\text{ M}\Omega\text{ cm}^2$, as could be expected from the presumably looser packing. At the same time, both membrane architectures showed typical capacitance values below $1\text{ }\mu\text{F cm}^{-2}$, indicative of the formation of a complete lipid bilayer. The lipid bilayers have then been exposed to a solution of α -hemolysin. This protein is known to form heptameric pores in lipid membranes, allowing for the flux of molecules across the

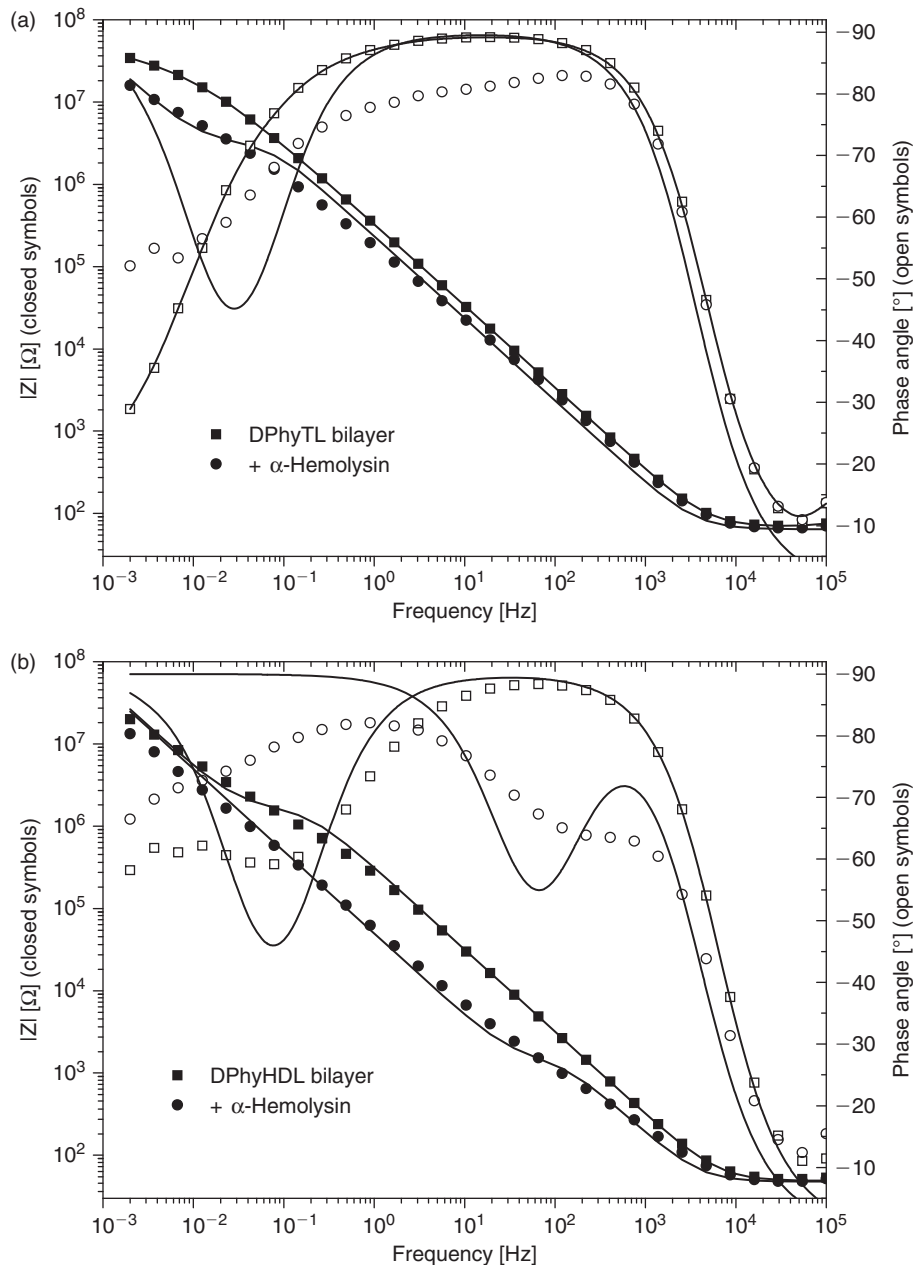


Fig. 7. Bode plots showing the incorporation of α -hemolysin into two different tBLM architectures. Solid lines represent fits to an R(RC)C equivalent circuit. The model has been kept consistent for all experiments in order to be able to compare the data, even though the deviations of the experimental data from the model increased, especially after protein incorporation.

bilayer.^[49,50] In electric measurements, this incorporation can be seen as a decrease in the membrane resistance. Indeed, in both the DPhyTL and the DPhyHDL-based tBLM systems, the addition of the protein (180 nM) resulted in a significant drop in the membrane resistance. The difference in the local structures of the two membrane architectures could be seen in the amplitude of this reduction. While the resistance for the DPhyTL-based membrane was reduced by about one order of magnitude to values of $1.5 \text{ M}\Omega \text{ cm}^2$, the resistance for DPhyHDL-based membranes decrease by a factor of ~ 2700 to values of $0.8 \text{ k}\Omega \text{ cm}^2$. Simultaneously, the capacitive values of the bilayers still showed the presence of a lipid bilayer leaflet. In order to be able to compare the obtained results, the electrical data has been analyzed using a simple equivalent circuit model,

as discussed above. However, the experimental data deviated significantly from the theoretical model once the protein was incorporated, especially in the case of DPhyHDL. This is probably because of the more inhomogeneous membrane architecture after the protein is embedded into the bilayer, which renders the whole system more complex. In fact, fitting the data using constant phase elements improves the quality of the fit results, however, it no longer allows for a quantified comparison of the data.

Conclusion

Tethered bilayer lipid membranes are useful model architectures that can be employed as a generic platform to study

membrane-related processes such as the functional incorporation of membrane proteins. Furthermore, they can be used as a sensing platform that can host engineered sensing peptides such as the here presented valinomycin derivatives. By being able to attach a selected binding group to the still functional depsi-peptide, a wide range of sensing possibilities can be envisioned. Here, as a proof of concept, the synthesis of a redox sensor has been shown.

The bare membrane architectures can also be used for sensing purposes. For example, the presence of membrane active peptides or proteins can be detected by monitoring changes in the electrical properties of the membrane. However, the intrinsic membrane architecture, i.e., the molecular structure of the anchor lipids used in the formation of the system, has a significant influence both on the properties of the membrane as well as on its ability to host membrane proteins.

Accessory Publication

Analytical data for ferrocene–valinomycin and EIS measurements are available on the Journal's website.

References

- [1] B. A. Cornell, V. L. B. Braach-Maksvytis, L. G. King, P. D. J. Osman, B. Raguse, L. Wiczorek, R. J. Pace, *Nature* **1997**, *387*, 580. doi:10.1038/42432
- [2] M. Winterhalter, *Curr. Opin. Colloid Interface Sci.* **2000**, *5*, 250. doi:10.1016/S1359-0294(00)00063-7
- [3] G. M. Bell, L. L. Combs, L. J. Dunne, *Chem. Rev.* **1981**, *81*, 15. doi:10.1021/CR00041A002
- [4] A. Ottova, V. Tvarozek, J. Racek, J. Sabo, W. Ziegler, T. Hianik, H. T. Tien, *Supramol. Sci.* **1997**, *4*, 101. doi:10.1016/S0968-5677(96)00054-5
- [5] E. Sackmann, *Science* **1996**, *271*, 43. doi:10.1126/SCIENCE.271.5245.43
- [6] C. Steinem, A. Janshoff, W.-P. Ulrich, M. Sieber, H.-J. Galla, *Biochim. Biophys. Acta* **1996**, *1279*, 169. doi:10.1016/0005-2736(95)00274-X
- [7] W. Knoll, C. W. Frank, C. Heibel, R. Naumann, A. Offenhäuser, J. Rühe, E. K. Schmidt, W. W. Shen, A. Sinner, *Rev. Mol. Biotechnol.* **2000**, *74*, 137. doi:10.1016/S1389-0352(00)00012-X
- [8] A. E. Vallejo, C. A. Gervasi, *Bioelectrochem* **2002**, *57*, 1. doi:10.1016/S1567-5394(01)00127-X
- [9] E. Sackmann, *Science* **1996**, *271*, 43. doi:10.1126/SCIENCE.271.5245.43
- [10] J. Spinke, J. Yang, H. Wolf, M. Liley, H. Ringsdorf, W. Knoll, *Biophys. J.* **1992**, *63*, 1667. doi:10.1016/S0006-3495(92)81742-3
- [11] L. K. Tamm, H. M. McConnell, *Biophys. J.* **1985**, *47*, 105. doi:10.1016/S0006-3495(85)83882-0
- [12] M. Winterhalter, *Curr. Opin. Colloid Interface Sci.* **2000**, *5*, 250. doi:10.1016/S1359-0294(00)00063-7
- [13] N. Fertig, A. Tilke, R. H. Blick, J. P. Kotthaus, J. C. Behrends, G. ten Bruggencate, *Appl. Phys. Lett.* **2000**, *77*, 1218. doi:10.1063/1.1289490
- [14] T. J. Jeon, N. Malmstadt, J. J. Schmidt, *J. Am. Chem. Soc.* **2006**, *128*, 42. doi:10.1021/JA056901V
- [15] I. K. Vockenroth, C. Ohm, J. W. F. Robertson, D. J. McGillivray, M. Lösche, I. Köper, *Biointerphases* **2008**, *3*, FA68. doi:10.1116/1.2912097
- [16] I. Köper, S. M. Schiller, F. Giess, R. Naumann, W. Knoll, *Adv. Planar Lipid Bilayers* **2006**, *3*, 37. doi:10.1016/S1554-4516(05)03002-4
- [17] S. M. Schiller, R. Naumann, K. Lovejoy, H. Kunz, W. Knoll, *Angew. Chem.* **2003**, *42*, 208. doi:10.1002/ANIE.200390080
- [18] S. Terrettaz, M. Mayer, H. Vogel, *Langmuir* **2003**, *19*, 5567. doi:10.1021/LA034197V
- [19] I. K. Vockenroth, P. P. Atanasova, A. T. A. Jenkins, I. Köper, *Langmuir* **2008**, *24*, 496. doi:10.1021/LA7030279
- [20] C. A. Keller, B. Kasemo, *Biophys. J.* **1998**, *75*, 1397. doi:10.1016/S0006-3495(98)74057-3
- [21] S. Terrettaz, H. Vogel, *MRS Bull.* **2005**, *30*, 207.
- [22] R. F. Roskamp, I. K. Vockenroth, N. Eisenmenger, J. Braunagel, I. Köper, *ChemPhysChem* **2008**, *9*, 1920. doi:10.1002/CPHC.200800248
- [23] R. Naumann, S. M. Schiller, F. Giess, B. Grohe, K. B. Hartman, I. Karcher, I. Köper, J. Lubben, K. Vasilev, W. Knoll, *Langmuir* **2003**, *19*, 5435. doi:10.1021/LA0342060
- [24] I. Köper, *Mol. Biosyst.* **2007**, *3*, 651. doi:10.1039/B707168J
- [25] I. K. Vockenroth, C. Rossi, M. R. Shah, I. Köper, *Biointerphases* **2009**, *4*, 19. doi:10.1116/1.3122019
- [26] J. Kunze, J. Leitch, A. L. Schwan, R. J. Faragher, R. Naumann, S. Schiller, W. Knoll, J. R. Dutcher, J. Lipkowski, *Langmuir* **2006**, *22*, 5509. doi:10.1021/LA0535274
- [27] A. Junghans, I. Köper, *Langmuir* **2010**, *26*, 11035. doi:10.1021/LA100342K
- [28] I. K. Vockenroth, C. Ohm, J. W. F. Robertson, D. J. McGillivray, M. Lösche, I. Köper, *Biointerphases* **2008**, *3*, FA68. doi:10.1116/1.2912097
- [29] H. Hillebrandt, M. Tanaka, E. Sackmann, *J. Phys. Chem. B* **2002**, *106*, 477. doi:10.1021/JP011693O
- [30] G. Stark, R. Benz, *J. Membr. Biol.* **1971**, *5*, 133. doi:10.1007/BF02107720
- [31] G. Favero, L. Campanella, A. D'Annibale, R. Santucci, T. Ferri, *Microchem. J.* **2003**, *74*, 141. doi:10.1016/S0026-265X(02)00179-0
- [32] B. Raguse, V. L. B. Braach-Maksvytis, B. A. Cornell, L. G. King, P. D. J. Osman, R. J. Pace, L. Wiczorek, *Langmuir* **1998**, *14*, 648. doi:10.1021/LA9711239
- [33] H. Brockmann, G. Schmidt-Kastner, I. Valinomycin, *Chem. Ber.* **1955**, *88*, 57. doi:10.1002/CBER.19550880111
- [34] M. M. Schemjakin, *Angew. Chem.* **1960**, *72*, 342. doi:10.1002/ANGE.19600721003
- [35] M. Rothe, W. Kreiss, *Angew. Chem. Int. Ed. Engl.* **1973**, *12*, 1012. doi:10.1002/ANIE.197310121
- [36] C. Gilon, Y. Klausner, A. Hassner, *Tetrahedron Lett.* **1979**, *20*, 3811. doi:10.1016/S0040-4039(01)95531-5
- [37] B. F. Gisin, A. R. Dhundale, *Int. J. Pept. Protein Res.* **1979**, *14*, 356. doi:10.1111/J.1399-3011.1979.TB01944.X
- [38] J. Hanzlík, Z. Samec, J. Hovorka, *J. Electroanal. Chem.* **1987**, *216*, 303. doi:10.1016/0022-0728(87)80217-6
- [39] B. Neises, W. Steglich, *Angew. Chem. Int. Ed. Engl.* **1978**, *17*, 522. doi:10.1002/ANIE.197805221
- [40] R. Naumann, D. Walz, S. M. Schiller, W. Knoll, *J. Electroanal. Chem.* **2003**, *550–551*, 241. doi:10.1016/S0022-0728(03)00013-5
- [41] G. Valincius, D. J. McGillivray, W. Febo-Ayala, D. J. Vanderah, J. J. Kasianowicz, M. Lösche, *J. Phys. Chem. B* **2006**, *110*, 10213. doi:10.1021/JP0616516
- [42] P. P. Atanasova, V. Atanasov, I. Köper, *Langmuir* **2007**, *23*, 7672. doi:10.1021/LA7002854
- [43] V. Atanasov, N. Knorr, R. S. Duran, S. Ingebrandt, A. Offenhäuser, W. Knoll, I. Köper, *Biophys. J.* **2005**, *89*, 1780. doi:10.1529/BIOPHYSJ.105.061374
- [44] I. K. Vockenroth, P. P. Atanasova, A. T. A. Jenkins, I. Köper, *Langmuir* **2008**, *24*, 496. doi:10.1021/LA7030279
- [45] L. H. He, J. W. F. Robertson, J. Li, I. Karcher, S. M. Schiller, W. Knoll, R. Naumann, *Langmuir* **2005**, *21*, 11666. doi:10.1021/LA051771P
- [46] D. J. McGillivray, G. Valincius, D. J. Vanderah, W. Febo-Ayala, J. T. Woodward, F. Heinrich, J. J. Kasianowicz, M. Lösche, *Biointerphases* **2007**, *2*, 21. doi:10.1116/1.2709308
- [47] J. A. Dura, D. J. Pierce, C. F. Majkrzak, N. C. Maliszewskyj, D. J. McGillivray, M. Lösche, K. V. O'Donovan, M. Mihailescu, U. Perez-Salas, D. L. Worcester, S. H. White, *Rev. Sci. Instrum.* **2006**, *77*, 074301. doi:10.1063/1.2219744
- [48] S. Krueger, C. W. Meuse, C. F. Majkrzak, J. A. Dura, N. F. Berk, M. Tarek, A. L. Plant, *Langmuir* **2001**, *17*, 511. doi:10.1021/LA001134T
- [49] B. Schuster, D. Pum, O. Braha, H. Bayley, U. B. Sleytr, *Biochim. Biophys. Acta* **1998**, *1370*, 208.
- [50] S. Cheley, M. S. Malghani, L. Song, M. Hobaugh, J. E. Gouaux, J. Yang, H. Bayley, *Protein Eng.* **1997**, *10*, 1433. doi:10.1093/PROTEIN/10.12.1433